

# First-principles simulation of cyanogen under high pressure: Formation of paracyanogen and an insulating carbon nitride solid

Mohammad Khazaei,\* Madhvendra Nath Tripathi, and Yoshiyuki Kawazoe

*Institute for Materials Research, Tohoku University, Sendai 980-8577, Japan*

(Received 15 December 2010; revised manuscript received 4 February 2011; published 8 April 2011)

Using a set of first-principles calculations, we have studied the phase transitions of cyanogen molecules ( $C_2N_2$ ) under high pressure. We obtained that at high pressure, cyanogen is transformed to a planar graphitelike structure with metallic property, which is experimentally known as paracyanogen. By increasing pressure, paracyanogen is transformed to an insulating carbon-nitrogen solid with an indirect band gap of 3.2 eV. Both above-mentioned phase transitions are first order and occur simultaneously with significant reduction in volumes. From our calculations, it is found that the planar structure of paracyanogen is made of ten-membered rings consisting of two C–C, four C–N, and four C=N bonds, while each carbon atom has  $sp^2$ -like hybridization. In the new-formed solid, all the carbon atoms have  $sp^3$ -like hybridization and all the nitrogen atoms have  $sp^2$ -like hybridizations with their nearest-neighbor C and N atoms. Our optical calculations show that cyanogen, which is a colorless gas, after above transitions turns to black paracyanogen polymer and then to a transparent solid. We have also used phonon dispersion calculation to show the stability of our predicted three-dimensional carbon-nitrogen system. Furthermore, it turns out that the predicted CN solid with stoichiometry 1:1 has also a good elastic property and a high bulk modulus of 330 GPa.

DOI: [10.1103/PhysRevB.83.134111](https://doi.org/10.1103/PhysRevB.83.134111)

PACS number(s): 61.50.Ks, 62.50.-p, 61.50.Ah, 61.66.Fn

## I. INTRODUCTION

Since after the theoretical prediction of Liu and Cohen for possible new hard materials based on carbon and nitrogen elements,<sup>1</sup> a lot of experimental and theoretical studies were devoted to the synthesis, characterization, modeling, and prediction of new crystalline, polymeric, and amorphous phases of carbon nitride, with different stoichiometries,  $C_1N_1$ ,<sup>2-7</sup>  $C_3N$ ,<sup>5,7,8</sup>  $C_3N_4$ .<sup>1,9-19</sup> Experimentally, carbon-nitride samples are synthesized using various carbon-nitrogen rich compounds, e.g., tetracyanoethylene, 1,3,5-tetrazine, paracyanogen,<sup>20-22</sup> and using various techniques such as high pressure, chemical vapor deposition, reactive sputtering, and laser ablation.<sup>17,21,23,24</sup> Theoretically, there are also several approaches for predicting new crystals or nanoclusters of carbon nitrides.<sup>2,5,25,26</sup> For example, some of the predictions are based on the previous known crystal structures. For instance, Côté and Cohen examined the existence of different crystal structures of carbon nitrides with stoichiometry 1:1 based on the crystal structures of GeP,  $\beta$ -InS, and GaSe.<sup>2</sup> As another way of prediction, the carbon atoms in the graphite structures are substituted with nitrogen atoms to reach particular  $C_xN_y$  compositions,<sup>8</sup> or the known inorganic compounds with rich nitrogen contents, such as paracyanogen, and tri-s-triazine,<sup>5,25,27</sup> are used as preliminary models. The hardness of the preliminary models can be further improved by applying external pressure or temperature<sup>5</sup> since it has already been demonstrated that high-pressure and -temperature techniques can represent an alternative approach to the synthesis of new polymers or solid systems.<sup>28-35</sup>

To search for new hard materials based on carbon and nitrogen elements, we previously studied the phase transitions of HCN molecules under high pressure, as it has experimentally been observed that HCN molecules are polymerized at high pressures.<sup>36</sup> From our calculations at high pressures, we

discovered several polymeric and layerlike structures of HCN, but not any with three-dimensional networks. This is due to the existing hydrogen element in our compound. We observed that hydrogen atoms always combine with available nitrogen and/or carbon atoms and prevent connection between the interlayers.<sup>37</sup> From the above calculations we obtained that for designing new carbon-nitride systems with three-dimensional networks, it is better to look for another inorganic compound, which includes only carbon and nitrogen atoms. In this regard, paracyanogen can be an ideal material. Therefore we decided to work on modification of paracyanogen by applying external pressure.

Concerning the crystal structure of paracyanogen, several suggested models are available,<sup>38-40</sup> shown in Fig. 1. All the experimental evidences support that paracyanogen has a planar lattice with very weak interlayer bonding and metallic behavior. However, unlike the graphite, it does not seem to have an extended delocalized  $\pi$  electron system.<sup>39</sup> To proceed our study, we have to know which of the structures in Fig. 1 can represent the real crystal structure of paracyanogen, although in many of the papers structure II has been assumed as a possible configuration for it.<sup>5</sup> To answer this question, we tried to analyze some of the available experimental data for the formation mechanism of paracyanogen. Experimentally, paracyanogen can be formed at high pressure from the cyanogen molecules. Yoo and Nicole suggested that at high pressure, initially the cyanogen molecules form a linear chain species, poly(2,3-diiminosuccinonitrile), which is very similar to structure I in Fig. 1, then the chain structures are connected and form paracyanogen polymers, structure II.<sup>41,42</sup>

To examine the procedure of phase transformation of cyanogen to paracyanogen at high pressure and to consider how by increasing pressure the planar structure of paracyanogen can be possibly transformed to a three-dimensional structure of carbon nitride, we have performed a set of first-principles calculations.

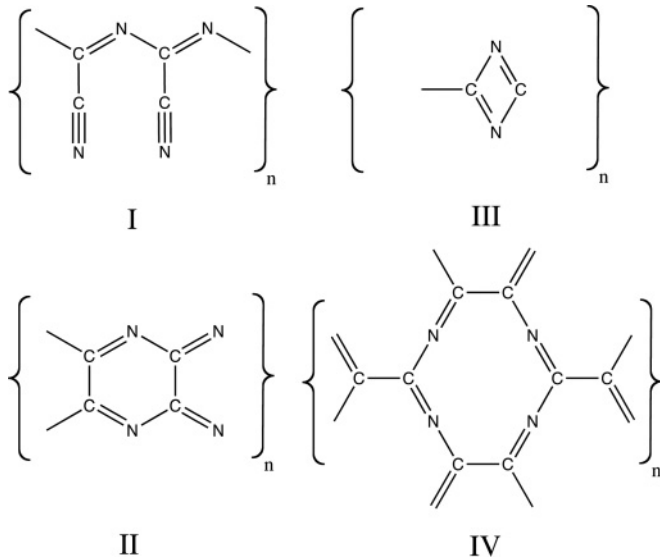


FIG. 1. Suggested crystal structures for paracyanogen in literature (Refs. 38–40).

## II. COMPUTATIONAL DETAIL

Cyanogen ( $C_2N_2$ ),  $N\equiv C-C\equiv N$ , is a colorless gas.<sup>38</sup> Its molecular crystal structure has already been determined experimentally at  $-95^\circ C$ . It is an orthorhombic structure with  $P_{cab}$  space group and lattice parameters of  $a = 6.31$ ,  $b = 7.08$ , and  $c = 6.19$  Å,<sup>43</sup> as shown in Fig. 2. Our calculations show that the crystal structures of cyanogen with  $P_{cab}$  and  $P_{bca}$  crystallographic group symmetries result in the same crystal structures with the same ground-state energies for cyanogen, but in different orientations. Since  $P_{bca}$  is the standard group space symmetry (no. 61), the sequence of lattice parameters in this paper are presented regarding this symmetry.

All the exploratory calculations are carried out within the context of density-functional theory (DFT) using the Perdew-Burke-Ernzerhof (PBE) exchange-correlation functional,<sup>44</sup> with the split valence double- $\zeta$  plus polarization orbitals basis set, and norm-conservative Troullier-Martins pseudopotential<sup>45</sup> as implemented in the SIESTA package program.<sup>46–48</sup> A real grid mesh with cutoff energy of 500 Ry is used to construct the electronic wave functions. The corresponding Brillouin zone is sampled by a set of  $6 \times 6 \times 6$  Monkhorst-Pack  $k$  points.<sup>49</sup> For structural optimizations, a variable-cell-shape conjugate gradient method under constant pressure is used without any constraint on symmetry. For finding the transitional structures, cell shape, volume, and atomic positions are optimized at the given pressure until the magnitude of force on each atom becomes smaller than  $0.005$  eV/Å. The stress tolerance is 1.0 GPa.

For the sake of assurance, we have examined the stability of the predicted structure at zero pressure by phonon dispersion calculation. The phonon frequencies are obtained by VIBRA, which is one of the utility packages of the SIESTA code. It calculates phonon frequencies and eigenmodes in a crystal, using the method of frozen phonons. To further examine the accuracy of the geometrical structures obtained from SIESTA calculations at ambient condition, we use a projected augmented wave (PAW) method at the same level of DFT theory

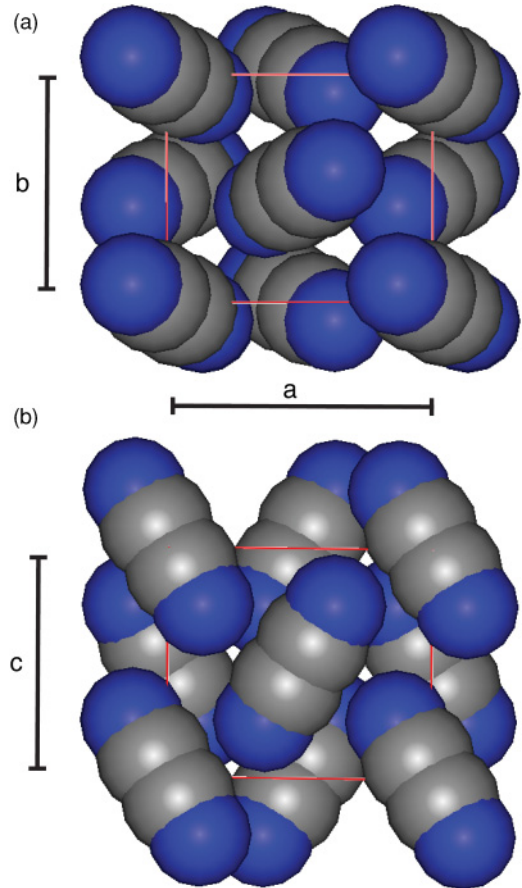


FIG. 2. (Color online) Unit cell of cyanogen with  $P_{bca}$  space group.  $a$ ,  $b$ , and  $c$  represent the lattice parameters. (a) and (b) show the  $ab$  and  $ac$  side views of the molecular crystal.

(PBE) using the VASP program.<sup>50</sup> For the PAW calculations, we have utilized a plane-wave cutoff energy of 520 eV.

Elastic constants are obtained based on the method proposed by Ravindran *et al.* for orthorhombic crystals.<sup>51</sup> For the elastic simulations, the necessary total-energy calculations are performed by VASP software. The bulk modulus is estimated by fitting of the curve of total energy versus volume to the third-order Birch-Murnaghan equation of states.<sup>52</sup>

The optical parameters are obtained from VASP calculations. In this regard, the real part of the dielectric function  $\epsilon_1(\omega)$  is calculated using the Kramers-Kronig transformation and the imaginary part of the optical dielectric function  $\epsilon_2(\omega)$  by summing the interband transitions from occupied to unoccupied states. Having obtained  $\epsilon_1(\omega)$  and  $\epsilon_2(\omega)$ , from complex dielectric function  $\epsilon(\omega) = \epsilon_1(\omega) + i\epsilon_2(\omega)$ , the transmittance  $T$  is then<sup>53,54</sup> computed with

$$T(\omega) = [1 - R(\omega)]e^{-\alpha(\omega)t}, \quad (1)$$

where,  $t$  is the thickness of the sample (in this study 150 nm). The reflection  $R(\omega)$  and absorption coefficient  $\alpha(\omega)$  are given by

$$R(\omega) = \left| \frac{\sqrt{\epsilon(\omega)} - 1}{\sqrt{\epsilon(\omega)} + 1} \right|^2, \quad (2)$$

$$\alpha(\omega) = 2(\omega) \left( \frac{[\epsilon_1^2(\omega) + \epsilon_2^2(\omega)]^{\frac{1}{2}} - \epsilon_1(\omega)}{2} \right)^{1/2}. \quad (3)$$

### III. RESULTS AND DISCUSSION

To simulate the phase transitions of the molecular structure of cyanogen under high pressure, we have used an orthorhombic structure with four cyanogen molecules per unit cell as experimentalists proposed it.<sup>43</sup> Table I shows the lattice and bond parameters of the optimized structure of cyanogen at ambient pressure (zero pressure) using SIESTA and VASP software in the same level of theory [DFT, generalized gradient approximation (GGA) with PBE functional] but with different basis sets, localized and plane wave. It is observed that SIESTA (VASP) under(over)estimates the lattice parameters. In both codes, at their present commercialized versions, the van der Waals interactions are neglected. This is one of the main reasons to justify the discrepancy of the obtained results from these first-principles codes in comparison with the experimental results at zero pressure. At higher pressures van der Waals interactions become less important, because the interactions are mainly chemical. However, VASP software gives better results for the bond distances and angles in comparison to SIESTA. Therefore first we have done all the exploratory calculations using SIESTA, which is due to having an efficient variable-cell-shape conjugate gradient algorithm for optimization under constant pressure, but when we want to discuss the electronic structure, optical properties, or elastic properties of the predicted structures, we have re-optimized the structures with VASP and present the results using this software. It should be noted that there is no significant difference between the electronic structure results obtained from SIESTA and VASP codes.

Figure 3 shows the pressure dependence of enthalpy, volume, and lattice parameters of the molecular crystal of cyanogen at zero temperature when external pressure changes from zero to 80 GPa. Enthalpy is defined as  $H = E_{\text{tot}} + PV$ , where  $E_{\text{tot}}$ ,  $P$ , and  $V$  are the total energy, pressure, and volume of the unit cell, respectively. It is observed that as the pressure increases two first-order phase transitions at 34 and 49 GPa occur, which are accompanied by heat releases, large volume reductions, and big changes in the lattice parameters.

TABLE I. Geometrical information of optimized structures using SIESTA and VASP software at ambient pressure in comparison to experimental results. All the distances are in Å and angles are in degrees.

Parameters	Experiment	SIESTA	VASP
$a$	$7.08 \pm 0.03$	6.522	7.44
$b$	$6.31 \pm 0.03$	5.596	6.82
$c$	$6.19 \pm 0.03$	5.632	6.50
C–C	$1.371 \pm 0.009$	1.394	1.373
C≡N	$1.131 \pm 0.015$	1.177	1.168
C–C≡N	$179.63 \pm 0.3$	177.9	179.92
botrule			

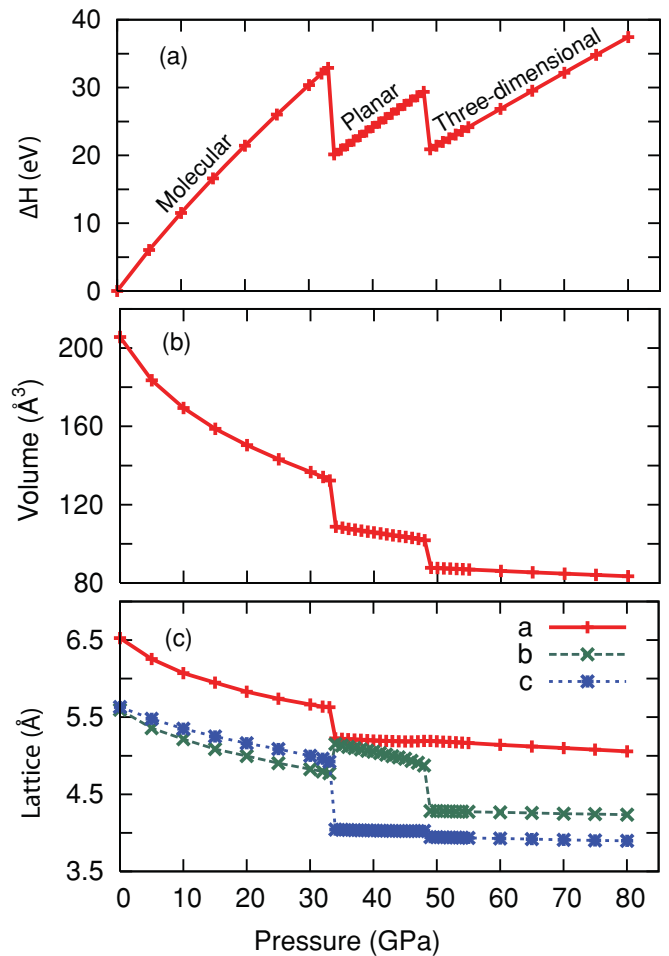


FIG. 3. (Color online) Pressure dependence of enthalpy (a), volume (b) and lattice parameters (c) unit cell of cyanogen with four molecules.

Figure 4 shows the geometrical structure of molecular crystal of cyanogen and the formed transitional structures at pressures 34 and 49 GPa. Our calculations show that after the first-order transitions the structural changes are irreversible and the transitional structures keep their shape at ambient pressure. As shown in Fig. 4, at 34 GPa the molecular structure of cyanogen is transformed to a planar graphitelike structure. At ambient condition, the distance between each two nearest carbon-nitride planes of the predicted structure is around 3.49 Å, which is very similar to interlayer distances,  $3.35 \pm 0.015$  Å,<sup>55</sup> between the carbon planes in graphite structure. However, in contrast to graphite with hexagonal carbon rings, our planar structure has ten-membered rings consisting of two C–C, four C–N, and four C=N bonds. All the carbon atoms have  $sp^2$ -like hybridizations with their nearest-neighboring atoms, one carbon and two nitrogen. The bond distances of C–C, C–N, and C=N are 1.49, 1.36, and 1.32 Å, respectively. All the nitrogen atoms have two carbon neighbors. The distance between the N–N lone pairs are 2.38 Å. The predicted structure has a  $P_{\text{bca}}$  space-group symmetry similar to the cyanogen molecular crystal.

In order to understand how the ten-membered rings with such particular compositions of carbon and nitrogen bonds are formed, see the side views of molecular crystal of

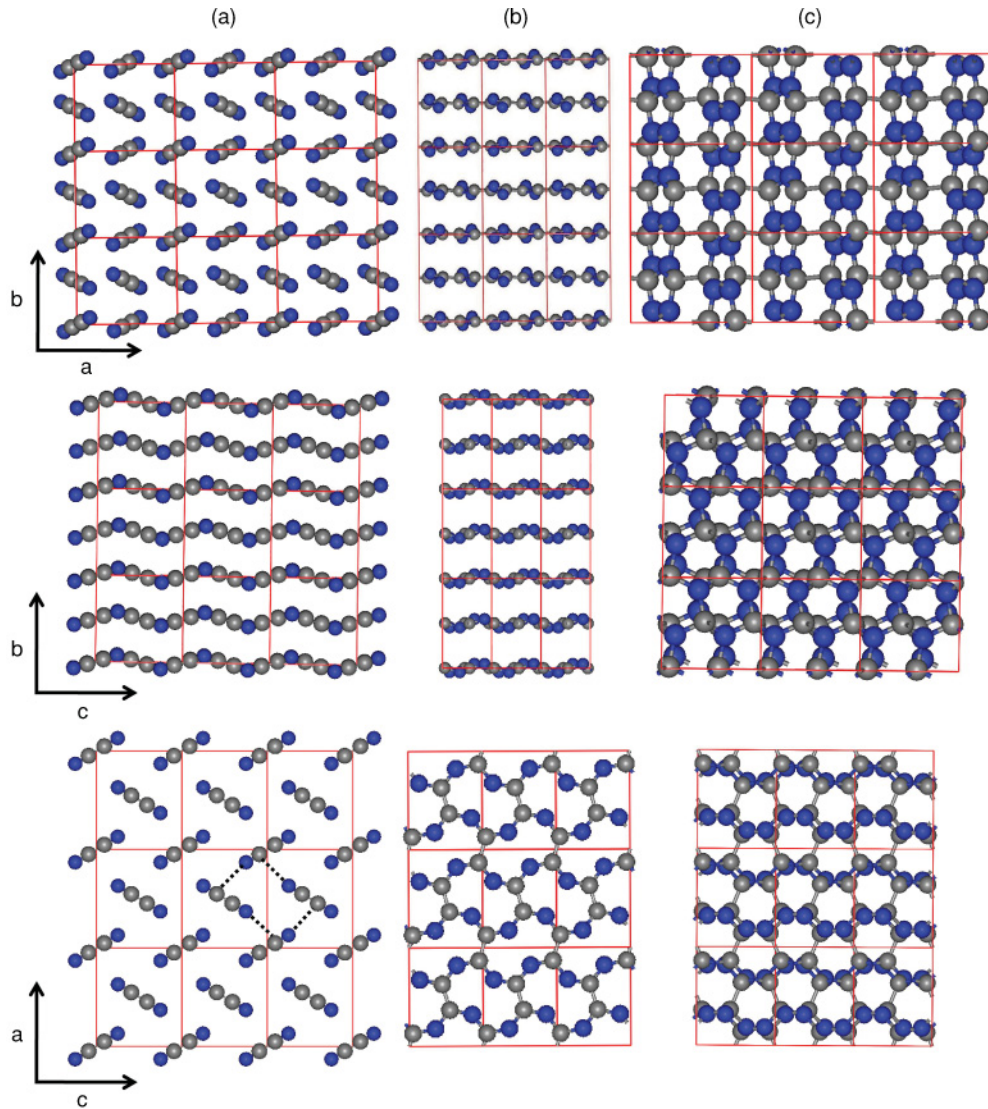


FIG. 4. (Color online) The columns show different side views ( $ab$ ,  $bc$ , and  $ac$ ) of the optimized structures at zero pressure for (a) molecular crystal of cyanogen, (b) the planar structure of paracyanogen formed at 34 GPa, and (c) the CN solid formed at 49 GPa. The dotted lines in (a) show schematically how the cyanogen molecules are interconnected to make the paracyanogen planes with ten-membered rings.

cyanogen shown in Fig. 4. It is observed that cyanogen has a layeredlike molecular crystal. As shown by dotted lines, under pressure each four cyanogen molecules on the same layer are combined together such that the ten-membered rings are formed. We believe that the predicted planar structure with ten-membered rings is probably the real structural configuration of paracyanogen. Our prediction is in agreement with the previously suggested model, structure IV shown in Fig. 1, by Bircumshaw *et al.* for paracyanogen.<sup>40</sup> More evidences are given below.

Experimentally paracyanogen can be formed at high pressure from cyanogen molecules<sup>41,42</sup> and has a planar lattice with very weak interlayer bonding but very strong interatomic bonding between the species on the same layer where carbon atoms have  $sp^2$ -like hybridization with other neighboring atoms. It can be seen that the predicted structure in this study has all above experimental signs of paracyanogen, i.e., it has been formed under high pressure and it has a planar

graphitelike structure (for further structural investigations, readers can find the  $xyz$  coordinate of our predicted structures in the supporting information file<sup>56</sup>). Experimentally, it was also indicated that paracyanogen is a metallic structure while unlike the graphite, it does not seem to have an extended delocalized  $\pi$  electron system.<sup>39</sup> In this regard, we have investigated the electronic structure of cyanogen molecules under pressure. Our calculations show that the molecular crystal of cyanogen has a very large energy gap 4.7 eV [see Fig. 5(a)], which by increasing pressure the energy gap decreases and at 34 GPa becomes a new metallic structure. Figure 5(b) shows the density of states of our predicted planar structure at ambient pressure. It is observed that it is a metallic structure as also experimentally found. All above evidences indicate that structure IV with ten-membered rings should be considered as one of the most likely candidates for the paracyanogen structure. It is worth mentioning that at ambient pressure our predicted paracyanogen structure is

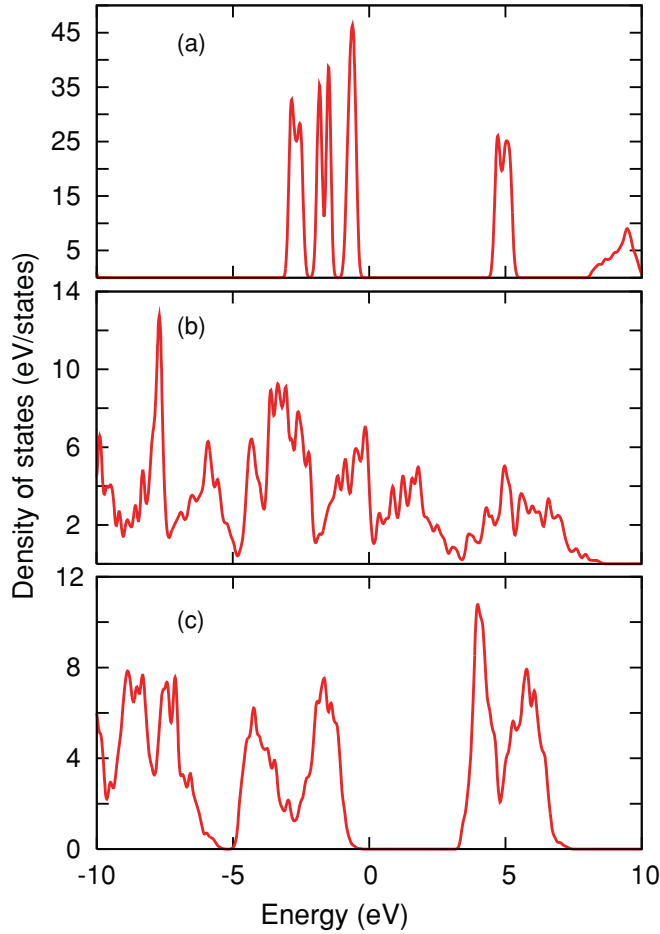


FIG. 5. (Color online) Total density of states for (a) cyanoen molecular crystal, (b) the predicted planar crystal (paracyanogen), and (c) the predicted three-dimensional CN-solid system at zero pressure. Fermi energy is at zero.

$-0.407$  eV/C<sub>2</sub>N<sub>2</sub> more stable than the molecular crystal of cyanogen.

To investigate the possibility of transformation of the planar structure of paracyanogen to a three-dimensional configuration, we applied higher external pressures. We found that under higher pressures, the planar layers of paracyanogen get close to each other such that at 49 GPa each carbon atom on

a plane makes a new bond with a nitrogen atom from the upper or lower plane. The new-formed three-dimensional CN solid is stable even if the external pressure is removed. It indicates that the transformation from paracyanogen to this CN solid is irreversible. The predicted CN solid has a  $P_{bca}$  space-group symmetry similar to paracyanogen and cyanogen molecular crystals. The mechanism of transformation of paracyanogen to the new CN crystal is very similar to the transformation mechanism of carbon graphite to hexagonal diamond structure.<sup>57</sup> In our predicted solid, all the carbon atoms have  $sp^3$ -like hybridization with their nearest-neighboring atoms, three nitrogen and one carbon atoms (the C–C and C–N bond distances are 1.68 and  $\sim 1.455$  Å, respectively), while all the nitrogen atoms have  $sp^2$ -like hybridization with their three nearest-neighboring carbon atoms. The performed phonon dispersion calculation (see the supplemental material<sup>56</sup>) shows that all the phonon frequencies are positive, which indicates that at ambient condition the predicted CN structure is stable and can exist. Also the total energy calculations show that our three-dimensional structure is energetically  $-0.374$  eV/C<sub>2</sub>N<sub>2</sub> more stable than cyanogen molecules. By comparing the stability of paracyanogen at ambient pressure with the formed three-dimensional CN system, it is seen that the CN solid is 0.033 eV/C<sub>2</sub>N<sub>2</sub> less stable than the paracyanogen structure. Therefore this might be expected that at very high temperature this CN solid turns to paracyanogen with graphitelike structure.

Table II shows the calculated elastic constants and bulk modulus of the designed CN solid in comparison to diamond. As a test calculation for our method, we have estimated the mechanical parameters of diamond in GGA and local-density approximation (LDA) and compared them to previous calculations and experimental results. The calculated parameters for diamond are in good agreement with the previous calculations.<sup>58,59</sup> By comparing the obtained parameters from calculations to the experimental ones,<sup>60,61</sup> it is found that GGA (LDA) functionals under(over)estimate the mechanical parameters. Hence in Table II the mechanical parameters of our CN solid are reported in both GGA and LDA. It is found that in our CN solid  $C_{22}$  and  $C_{33}$  are larger than  $C_{22}$  and  $C_{33}$  of carbon diamond, but its  $C_{11}$  is less. The above behavior can be attributed to the shorter covalent C–N bond distances (which are mainly oriented along the 010 and 001 directions) and the longer covalent C–C bond distances

TABLE II. Calculated elastic constants  $C_{ij}$  (GPa) and bulk modulus  $B$  (GPa) for diamond and our predicted three-dimensional CN solid. T. and P. stand for this and previous studies. In diamond due to symmetries  $C_{22}$  and  $C_{33}$  are equal with  $C_{11}$ .  $C_{13}$  and  $C_{23}$  are equal with  $C_{12}$ .

Material	Method	$C_{11}$	$C_{12}$	$C_{13}$	$C_{22}$	$C_{23}$	$C_{33}$	$C_{44}$	$C_{55}$	$C_{66}$	$B$
C-diamond	T. GGA	1052.5	126.0					563.8			434.1
	T. LDA	1109.3	144.6					608.2			465.9
	P. GGA	1053 <sup>a</sup>	127.0 <sup>a</sup>					565.0 <sup>b</sup>			424.0 <sup>b</sup>
	P. LD	1106.0 <sup>a</sup>	151.0 <sup>a</sup>					604.0 <sup>a</sup>			458.0 <sup>a</sup>
	Expt.	$1076.4 \pm 0.2^c$	$125.2 \pm 2.3^c$					$577.4 \pm 1.4^c$			443.0 <sup>d</sup>
CN	T. GGA	543.2	161.8	134.5	1089.0	125.8	1165.5	472.4	369.6	308.7	330.4
	T. LDA	617.2	186.5	143.0	1200.9	141.5	1273.6	517.5	392.0	336.4	375.7

<sup>a</sup>Reference 58.

<sup>b</sup>Reference 59.

<sup>c</sup>Reference 60.

<sup>d</sup>Reference 61.

(which are mainly oriented along the 100 direction) in our predicted solid than the C–C bonds (1.57 Å) in diamond. It is worth mentioning that Cohen predicted that materials which are made of carbon and nitrogen exhibit a bulk modulus higher than diamond due to the short length of the C–N bond.<sup>62</sup> In this regard, we have calculated the bulk modulus (330 GPa) of our three-dimensional solid. It is found that our designed CN solid due to having C–C bonds, which are longer than the C–C bonds in diamond, cannot be harder than diamond structure, but still it has better/comparable elastic constants and bulk modulus than/with many of the other predicted carbon-nitrogen crystals.<sup>2–4</sup>

Figure 5(c) shows the density of states of the predicted CN system. The electronic structure calculations indicate that our CN solid is an insulator with an indirect band gap of 3.2 eV (see the band structure in the supplemental material<sup>56</sup>). It is known that DFT/GGA calculations underestimate the band gap. Therefore it is expected that the experimental value for the band gap will be larger by several eV. For  $\beta$ -C<sub>3</sub>N<sub>4</sub> structure, it has also been reported that it has a very large indirect band gap, 6.75 eV, estimated by GW approximation.<sup>63</sup> It is also worth mentioning that among the CN solids with the same stoichiometry 1:1 (whose electronic structures have already been reported in the literature), our CN solid has the largest band gap. Most of the other predicted CN solids are metallic<sup>2,3</sup> or they are semiconductors with very small band gaps.<sup>4</sup>

In order to investigate the pressure dependence of optical properties of cyanogen molecules and the related transitional configurations, we have calculated the transmittance curves of our structures under different pressures, shown in Fig. 6. It is observed that by increasing the applied pressure, the transmittance of the molecular crystal of cyanogen decreases and when the metallic paracyanogen is formed, the transmittance becomes almost zero in the visible wavelength region,

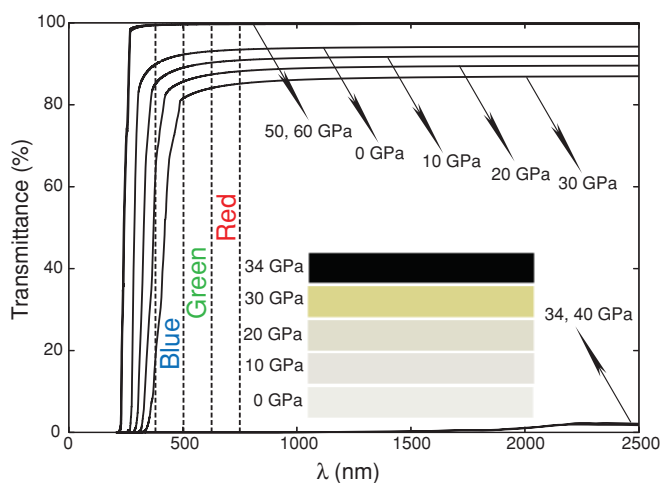


FIG. 6. (Color online) Pressure dependence of transmittance. The dotted lines indicate the visible optical window between 380 and 750 nm with mixture of blue, green, and red colors. The inset shows how under pressure <34 GPa, the color of molecular crystal of cyanogen changes from colorless to brownlike. At pressures between 34 and 50 GPa, the material is completely black. At pressures  $\geq 50$  GPa, it is completely transparent.

shown by dotted lines. In Fig. 6 it is also shown how the color of cyanogen changes under pressure. The colors are approximately calculated from the mixture of the average of the transmittance in the blue, green, and red regions. It is observed that cyanogen at ambient condition is a colorless gas but by applying external pressure, it becomes brownish and when the paracyanogen is formed, it becomes completely black. Our calculated optical spectra is in accordance to the experimental observations that at pressures above 6 GPa, the cyanogen sample develops a deep yellow-brown hue which deepens slowly with increasing pressure until 10 GPa, where the samples turn black rapidly. At pressures above 10 GPa, cyanogen molecules are transformed to a black polymer, which is chemically and thermally stable (paracyanogen).<sup>41</sup> Moreover, our optical calculations show that when by increasing pressure the two-dimensional structure of paracyanogen is transformed to a three-dimensional CN system, the resultant CN solid is completely transparent due to its very large band gap.

In order to consider the effect of supercell size in the simulations, we have repeated the calculations at near transition pressures by using supercells consisting of 32 cyanogen molecules, which are eight times larger than the initial unit cell that was used at the beginning. However, from the above calculations we could not find any new phase transition except those phases that we have already discussed.

All the calculations in this study were carried out at zero temperature, which results in overestimation of transitional pressures in our simulation in comparison to experiment. For example, in our calculations paracyanogen is formed at 34 GPa, while Yoo and Nicole observed it at pressures above 10 GPa at their experiments. To understand the reason why phase transition pressures are overestimated in the first-principles simulations, both experimental conditions and theoretical limitations should be taken into account. It is seen that in the experiments, the cyanogen samples are kept at the above-mentioned pressure and at 297 K for several hours.<sup>41,42</sup> Therefore the kinetics of phase formations become an important issue, which is not treated well in the first-principles simulations. This is because performing molecular-dynamics simulations as for as long a time as the time scales of experiments using first-principles approaches is very expensive and practically impossible. Another reason concerning why the transition pressures are overestimated in the typical constant-pressure *ab initio* simulations is that in these simulations the structural phase transformations do not proceed by nucleation and growth, but instead they occur across the entire simulation cell. As a result, systems have to cross a significant energy barrier to transform from one phase to another and hence the simulation box has to be overpressurized in order to obtain a phase transition.<sup>64,65</sup> Overestimation of pressure in first-principles simulations might also be expected due to some intrinsic problems of DFT. In this regard, we can point to the inaccuracy of DFT in evaluation of energy barriers for bond formations or  $\pi \rightarrow \sigma$  transformations.<sup>66–68</sup> In typical conjugated systems, DFT also overestimates the torsional energy barriers.<sup>69,70</sup>

It should be noted that experimentally it was found that before the formation of paracyanogen, cyanogen molecules reversibly convert to a linear chain of dimers,  $(-(C_2N_2)_2-)_m$ ,<sup>41</sup>

which was not observed in our simulations. We cannot exclude the possibility of existence of this phase in the experiment, because in our simulations the effects of time and temperature have not been included. In the range of pressures  $< 80$  GPa applied in this study, we have not seen any other phase transition. However, at very extreme pressure conditions new phase transitions might be possible. In this regard, Sun *et al.* have shown that there is a structural transformation for even diamond at pressures around 2.5 TPa.<sup>71</sup>

In the literature, there are many suggested crystal structures for carbon nitride systems. Recently Hart *et al.* have performed an extensive study on relative stabilities of different phases of carbon nitride systems with the same stoichiometries.<sup>5</sup> They have predicted two CN structures with lowest energies with stoichiometry 1:1, labeled structures *B* and *D* in their paper.<sup>5</sup> Structure *D* is a planar-ribbon-like configuration and structure *B* is a three-dimensional carbon nitride system ( $\beta$ -InS-like). In order to compare the relative stabilities of our designed structures, we have compared the total energy of our structures with energies of structures *B* and *D*. It is observed that structure *D* (0.0 eV/atom)  $<$  structure *B* (0.12 eV/atom)  $<$  the planar paracyanogen (0.29 eV/atom)  $<$  the three-dimensional CN (0.30 eV/atom). It is seen that our structures are not the most stable phases of the carbon nitrides. This calculation also shows that the planar-ribbon-like structure *D*, is more stable than the three-dimensional structure *B*, which is consistent with our observation as discussed earlier, that paracyanogen with planar structure is more stable than that of the three-dimensional system. Furthermore, similarly it has been reported that graphite is slightly ( $-2.9$  KJ/mol) more stable than diamond.<sup>15</sup>

In addition to cyanogen, there are several studies on the effect of high pressure on other types of inorganic molecules which consist of carbon and nitrogen atoms so as to synthesize crystalline carbon nitride solids.<sup>72-80</sup> For example, Aoki *et al.* have reported the polymerization of cyanoacetylene under

pressures above 1.5 GPa.<sup>72</sup> Nesting and Badding have reported the synthesis of amorphous  $sp^2$ -bonded and crystalline  $sp^3$ -bonded carbon nitrides from tetracyanoethylene in a diamond-anvil cell.<sup>76</sup>

#### IV. CONCLUSION

In the present first-principles study, we have considered the high-pressure phases of cyanogen molecules. It is found that by increasing pressure, the cyanogen molecules are transformed to a metallic graphiticlike structure (paracyanogen) and at higher pressures, paracyanogen is transformed to an insulator with three-dimensional C–C and C–N networks. It is observed that the structural planar configuration of paracyanogen is made of ten-membered rings consisting of two C–C, four C–N, and four C=N bonds while all the carbon atoms have  $sp^2$ -like hybridization. In the predicted CN solid, all the carbon and nitrogen atoms have  $sp^3$ - and  $sp^2$ -like hybridization with other neighboring carbon and nitrogen atoms, respectively. From our optical calculations, it is found that paracyanogen is a black material, while the CN solid is completely transparent. The latter structure has also a very good elastic property and high bulk modulus in comparison to other predicted carbon-nitride solids.

#### ACKNOWLEDGMENTS

The authors sincerely thank the crew of the Center for Computational Materials Science of the Institute for Materials Research, Tohoku University, for their continuous support of the supercomputing facilities. Also we thank A. Šimůnek, A. Ranjbar, and P. K. Nandi for their fruitful discussions. M.K. thanks the Japan Society for the Promotion of Science (JSPS) for financial support.

\*khazaei@imr.edu

<sup>1</sup>A. Y. Liu and M. L. Cohen, *Science* **245**, 841 (1989).

<sup>2</sup>M. Côté and M. L. Cohen, *Phys. Rev. B* **55**, 5684 (1997).

<sup>3</sup>X. Wang, K. Bao, F. Tian, X. Meng, C. Chen, B. Dong, D. Li, B. Liu, and T. Cui, *J. Chem. Phys.* **133**, 044512 (2010).

<sup>4</sup>E. Kim, C. Chen, T. Köhler, M. Elstner, and T. Frauenheim, *Phys. Rev. B* **64**, 094107 (2001).

<sup>5</sup>J. N. Hart, F. Claeysens, N. L. Allan, and P. W. May, *Phys. Rev. B* **80**, 174111 (2009).

<sup>6</sup>G. Chai, C. Lin, M. Zhang, J. Wang, and W. Cheng, *J. Phys.: Condens. Matter* **21**, 144203 (2009).

<sup>7</sup>J. Hales and A. S. Barnard, *J. Phys.: Condens. Matter* **21**, 144203 (2009).

<sup>8</sup>E. Sandré, C. J. Pickard, and C. Colliex, *Chem. Phys. Lett.* **325**, 53 (2000).

<sup>9</sup>K. M. Yu, M. L. Cohen, E. E. Haller, W. L. Hansen, A. Y. Liu, and I. C. Wu, *Phys. Rev. B* **49**, 5034 (1994).

<sup>10</sup>D. M. Tetr and R. J. Hemley, *Science* **271**, 53 (1996).

<sup>11</sup>A. Y. Liu and R. M. Wentzcovitch, *Phys. Rev. B* **50**, 10362 (1994).

<sup>12</sup>Y. Peng, T. Ishigaki, and S. Horiuchi, *Appl. Phys. Lett.* **73**, 3671 (1998).

<sup>13</sup>P. H. Fang, *J. Mater. Sci. Lett.* **14**, 536 (1995).

<sup>14</sup>Z. J. Zhang, J. Huang, S. Fan, and C. M. Lieber, *Mater. Sci. Eng. A* **209**, 5 (1996).

<sup>15</sup>J. V. Badding, *Adv. Mater.* **9**, 877 (1997).

<sup>16</sup>S.-D. Mo, L. Ouyang, W. Y. Ching, I. Tanaka, Y. Koyama, and R. Riedel, *Phys. Rev. Lett.* **83**, 5046 (1999).

<sup>17</sup>Y. Chen, L. Guo, F. Chen, and E. G. Wang, *J. Phys.: Condens. Matter* **8**, L685 (1996).

<sup>18</sup>H. Montigaud, B. Tanguy, G. Demazeau, I. Alves, M. Birot, and J. Dunogues, *Diam. Relat. Mater.* **8**, 1707 (1999).

<sup>19</sup>C. Niu, Y. Z. Lu, and C. M. Lieber, *Science* **261**, 334 (1993).

<sup>20</sup>T. Sekine, H. Kanda, Y. Bando, and M. Yokoyama, *J. Mater. Sci. Lett.* **9**, 1376 (1990).

<sup>21</sup>A. J. Stevens, T. Koga, C. B. Agee, M. J. Aziz, and C. M. Lieber, *J. Am. Chem. Soc.* **118**, 10900 (1996).

<sup>22</sup>A. J. Stevens, C. B. Agee, and C. M. Lieber, *Mater. Res. Soc. Symp. Proc.* **499**, 309 (1998).

<sup>23</sup>E. G. Wang, *Prog. Mater. Sci.* **41**, 241 (1998).

<sup>24</sup>S. Muhl and J. M. Méndez, *Diam. Relat. Mater.* **8**, 1809 (1999).

<sup>25</sup>G. Román-Pérez, F. Zamora, and J. M. Soler, *Phys. Rev. B* **82**, 195405 (2010).

- <sup>26</sup>M. M. Al Mogren, A. A. El-Azhary, and W. Alkiali, *J. Phys. Chem. A* **114**, 12258 (2010).
- <sup>27</sup>A. Thomas, A. Fischer, F. Goettman, M. Antonietti, J.-O. Müller, R. Schlögl, and J. M. Carlsson, *J. Mater. Chem.* **18**, 4893 (2008).
- <sup>28</sup>R. J. Hemley, *Annu. Rev. Phys. Chem.* **51**, 763 (2000).
- <sup>29</sup>M. Citroni, M. Ceppatelli, R. Bini, and V. Schettino, *Science* **15**, 2058 (2002).
- <sup>30</sup>L. Ciabini, M. Santoro, F. A. Gorelli, R. Bini, V. Schettino, and S. Raugei, *Nat. Mater.* **6**, 39 (2007).
- <sup>31</sup>D. Chelazzi, M. Ceppatelli, M. Santoro, R. Bini, and V. Schettino, *Nat. Mater.* **3**, 470 (2004).
- <sup>32</sup>V. Schettino and R. Bini, *Chem. Soc. Rev.* **36**, 869 (2007).
- <sup>33</sup>V. Schettino and R. Bini, *Phys. Chem. Chem. Phys.* **5**, 1951 (2003).
- <sup>34</sup>X.-F. Zhou, G.-R. Qian, X. Dong, L. Zhang, Y. Tian, and H.-T. Wang, *Phys. Rev. B* **82**, 134126 (2010).
- <sup>35</sup>K. Iyakutti, M. Rajarajeswari, and Y. Kawazoe, *Physica B* **405**, 3324 (2010).
- <sup>36</sup>K. Aoki, B. J. Baer, H. C. Cynn, and M. Nicol, *Phys. Rev. B* **42**, 4298 (1990).
- <sup>37</sup>M. Khazaei, M. S. Bahramy, F. Picherri, K. Esfarjani, and Y. Kawazoe (unpublished).
- <sup>38</sup>T. K. Brotherton and J. W. Lynn, *Chem. Rev.* **59**, 841 (1959).
- <sup>39</sup>L. Maya, *J. Polym. Sci., Part A: Polym. Chem.* **31**, 2595 (1993).
- <sup>40</sup>L. L. Bircumshaw, F. M. Tayler, and D. H. Whiffen, *J. Chem. Soc.* **931** (1954).
- <sup>41</sup>C.-S. Yoo and M. Nicol, *J. Phys. Chem.* **90**, 6726 (1986).
- <sup>42</sup>C.-S. Yoo and M. Nicol, *J. Phys. Chem.* **90**, 6732 (1986).
- <sup>43</sup>A. S. Parkes and R. E. Hughes, *Acta Crystallogr.* **16**, 734 (1963).
- <sup>44</sup>J. P. Perdew, K. Burke, and M. Ernzerhof, *Phys. Rev. Lett.* **77**, 3865 (1996).
- <sup>45</sup>N. Troullier and J. L. Martins, *Phys. Rev. B* **43**, 1993 (1991).
- <sup>46</sup>P. Ordejón, E. Artacho, and J. M. Soler, *Phys. Rev. B* **53**, R10441 (1996).
- <sup>47</sup>J. M. Soler, E. Artacho, J. D. Gale, A. García, J. Junquera, P. Ordejón, and D. Sánchez-Portal, *J. Phys.: Condens. Matter* **14**, 2745 (2002).
- <sup>48</sup>D. Sánchez-Portal, E. Artacho, and J. M. Soler, *J. Phys.: Condens. Matter* **8**, 3859 (1996).
- <sup>49</sup>H. J. Monkhorst and J. D. Pack, *Phys. Rev. B* **13**, 5188 (1976).
- <sup>50</sup>G. Kresse and J. Furthmüller, *Comput. Mater. Sci.* **6**, 15 (1996).
- <sup>51</sup>P. Ravindran, L. Fast, P. A. Korzhavyi, B. Johansson, J. Wills, and O. Eriksson, *J. Appl. Phys.* **84**, 4891 (1998).
- <sup>52</sup>Y. Liang and Z. Fang, *J. Phys.: Condens. Matter* **18**, 8749 (2006).
- <sup>53</sup>P. Ravindran, A. Delin, B. Johansson, O. Eriksson, and J. M. Wills, *Phys. Rev. B* **59**, 1776 (1999).
- <sup>54</sup>S. A. Knickerbocker and A. K. Kulkarni, *J. Vac. Sci. Technol. A* **13**, 1048 (1995).
- <sup>55</sup>H.-K. Jeong, H.-J. Noh, J.-Y. Kim, M. H. Jin, C. Y. Park, and Y. H. Lee, *Europhys. Lett.* **82**, 67004 (2008).
- <sup>56</sup>See supplemental material at [<http://link.aps.org/supplemental/10.1103/PhysRevB.83.134111>] for the coordinates of the predicted structures, phonon dispersion, and band structure of the CN solid, and the xyz trajectory files of phase transformations.
- <sup>57</sup>J. Sung, *J. Mater. Sci.* **35**, 6041 (2000).
- <sup>58</sup>Y. Liang, W. Zhang, J. Zhao, and L. Chen, *Phys. Rev. B* **80**, 113401 (2009).
- <sup>59</sup>Y. Liang and W. Zhang, and L. Chen, *Europhys. Lett.* **87**, 56003 (2009).
- <sup>60</sup>M. H. Grimsditch and A. K. Ramdas, *Phys. Rev. B* **11**, 3139 (1975).
- <sup>61</sup>M. T. Yin, *Phys. Rev. B* **30**, 1773 (1984).
- <sup>62</sup>M. L. Cohen, *Phys. Rev. B* **32**, 7988 (1985).
- <sup>63</sup>J. L. Corkill and M. L. Cohen, *Phys. Rev. B* **48**, 17622 (1993).
- <sup>64</sup>M. Durandurdu, *Phys. Rev. B* **75**, 235204 (2007).
- <sup>65</sup>K. Mizushima, S. Yip, and E. Kaxiras, *Phys. Rev. B* **50**, 14952 (1994).
- <sup>66</sup>S. N. Pieniazek, F. R. Clemente, and K. Houk, *Angew. Chem. Int. Ed.* **47**, 7746 (2008).
- <sup>67</sup>P. R. Schreiner, *Angew. Chem. Int. Ed.* **46**, 4217 (2007).
- <sup>68</sup>S. E. Wheeler, A. Moran, S. N. Pieniazek, and N. Houk, *J. Phys. Chem. A* **113**, 10376 (2009).
- <sup>69</sup>A. Karpfen, C. H. Choi, and M. Kertesz, *J. Phys. Chem. A* **101**, 7426 (1997).
- <sup>70</sup>B. Mannfors, J. T. Koskinen, L.-O. Pietilä, and L. Ahjopalo, *J. Mol. Struct.* **393**, 39 (1997).
- <sup>71</sup>J. Sun, D. D. Klug, and R. Martoňák, *J. Chem. Phys.* **130**, 194512 (2009).
- <sup>72</sup>K. Aoki, Y. Kalkudate, M. Yoshida, S. Usuba, and S. Fujiwara, *J. Chem. Phys.* **91**, 778 (1989).
- <sup>73</sup>H. G. Drickamer, *Science* **156**, 1183 (1967).
- <sup>74</sup>T. R. Ravindran and J. V. Badding, *J. Mater. Sci.* **41**, 7145 (2006).
- <sup>75</sup>J. V. Badding and D. C. Nesting, *Chem. Mater.* **8**, 535 (1996).
- <sup>76</sup>D. C. Nesting and J. V. Badding, *Chem. Mater.* **8**, 1535 (1996).
- <sup>77</sup>J. V. Badding, L. J. Parker, and D. C. Nesting, *J. Solid State Chem.* **117**, 229 (1995).
- <sup>78</sup>E. Horvath-Bordon, R. Riedel, P. F. McMillan, P. Kroll, G. Miehe, P. A. van Aken, A. Zerr, P. Hoppe, O. Shebanova, I. McLaren, S. Lauterbach, E. Kroke, and R. Boehler, *Angew. Chem.* **46**, 1476 (2007).
- <sup>79</sup>P. F. McMillan, V. Less, E. Quirico, G. Montagnac, A. Sella, B. Reynard, P. Simon, E. Bailey, M. Deifallah, and F. Corà, *J. Solid State Chem.* **182**, 2670 (2009).
- <sup>80</sup>Z. Zhang, K. Leinenweber, M. Bauer, L. A. J. Garvie, P. F. McMillan, and G. H. Wolf, *J. Am. Chem. Soc.* **123**, 7788 (2001).